Optical modes in mesoscopic quantum cascade ring lasers

S. Anders, V. Tamosiunas, W. Schrenk, and G. Strasser
Institut für Festkörperelektronik, Technische Universität Wien, A-1040 Wien, Austria
(Received 19 May 2003; revised manuscript received 29 August 2003; published 20 February 2004)

We present lasing spectra of mesoscopic rings processed from a GaAs-based quantum cascade material. The emission properties are investigated for various inner ring radii. Small inner radii leave the spectra unaffected, whereas large inner radii shift the spectra to smaller wavelengths. To obtain insight into the spatial distribution of the optical modes, we performed simulations with a finite-difference time-domain method.

DOI: 10.1103/PhysRevB.69.073309 PACS number(s): 78.20.−e, 42.55.−f

Ring-shaped resonators have been investigated for both optical applications and basic research. For example, they are of interest as compact building blocks for optical signal processing.[1–3] Here, the ring served as resonator. Evanescent-wave coupling of a ring-shaped gain medium separated from the resonator has been demonstrated as well.[4] The ring can also serve as both gain medium and resonator, with a ring material of, for example, a semiconducting polymer,[5] InGaAs single quantum wells,[6] InGaN/GaN multiple quantum wells,[7] and InGaAsP quantum wells.[8] All of these devices were optically pumped. For the work described in the following, we investigated electrically pumped ring lasers. They were processed from a GaAs/AlGaAs heterostructure that was designed for quantum cascade lasing in the midinfrared.

Devices related to such ring lasers are cylinder- or disk-shaped quantum cascade lasers (QCLs).[9–11] Compared to ridge-shaped lasers, the optical interface losses for circular cavities are potentially decreased. Ideally, the modes propagate as whispering gallery modes and suffer losses only by evanescent leakage. A surface that is sufficiently smooth and substantially reduces losses compared to ridge cavities may be processed, for example, by reactive ion etching. Such devices have already demonstrated room temperature lasing at 12.6 μm.[12] Intentionally deformed cavities have the advantage that a larger fraction of the emitted light is collectable.[10,13,14]

The aim of this work is to demonstrate that ring lasers based on a quantum cascade material are functional, and to gain knowledge about the spatial mode distribution in the ring lasers. To this end, we processed rings with various inner radii while the outer radius was kept fixed at three different values, 100, 150, and 200 μm. By measuring spectral properties of the rings, we can infer how far the modes extend toward the ring center. We further performed simulations with the body of revolution finite-difference time-domain method to obtain the spatial mode distribution.

The ring cavities were processed from a GaAs/AlGaAs heterostructure. The active area, injector, and waveguide were grown by solid source molecular beam epitaxy on doped n^+ GaAs (100) substrates with a doping concentration of $n_{si}=2\times10^{18}$ cm^{-3}. $Al_{0.45}Ga_{0.55}As$ was used for both the barriers in the active region and in the injector. The conduction band discontinuity at the Γ point is $\Delta E_c \approx 390$ meV. Forty active area/injector stages were cascaded. Starting with the injector barrier, one stage consists of [**AlGaAs** (**nm**)/GaAs (nm)]: **2.6**/3.0/**2.0**/2.8/**1.8**/3.0/**1.7**/3.4/**2.8**/4.8/**1.1**/5.4/**1.1**/1.9/**4.6**/3.0. Underlined layers are doped. Because the optical transition is based on an intersubband transition between quantized conduction band states, only TM polarized light is allowed. Thus, since the polarization is normal to the layers, no light is lost through the top and bottom of the rings. Data from the same material, processed as a Fabry-Pérot ridge cavity, have been shown elsewhere.[15]

The waveguides of the ring lasers were defined by reactive ion etching. Patterned SiN was used as the etch mask. A relatively high power of the $SiCl_4$ plasma, 160 W at 4 mtorr, resulted in a perpendicular and smooth ring boundary. Figure 1 shows a scanning electron microscope (SEM) image of a ring laser. To allow for bonding, a Ti/Au metallization was sputtered on top of the cavity. Typically, two bonding wires were positioned on the cavity. To check if an inhomogeneous current distribution caused by the particular position of the bonding wires affects the properties of the ring lasers, we bonded from one to seven wires on one ring. In terms of threshold, spectral output, and maximum operation temperature, no trend was found. However, cylinder-shaped lasers with two peripheral bonding wires had a higher optical output than a device with one central bonding wire. Further, the spectra of cylinders with two bonding wires were more irregular than the spectra of cylinders with one central bonding wire. The envelope of the spectra was not systematically altered.

The threshold of the ring lasers at 78 K is between 3.5 and 7 kA/cm^2. Fabry-Pérot cavities from the same material have a threshold down to 3 kA/cm^2. The relatively large scatter of

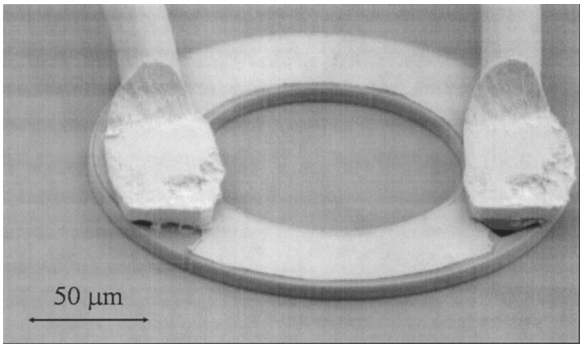

FIG. 1. SEM image of a ring laser bonded with two wires. The top metallization (partly ripped off by the bonding wires) is visible. The height of the ring is approximately 10 μm.

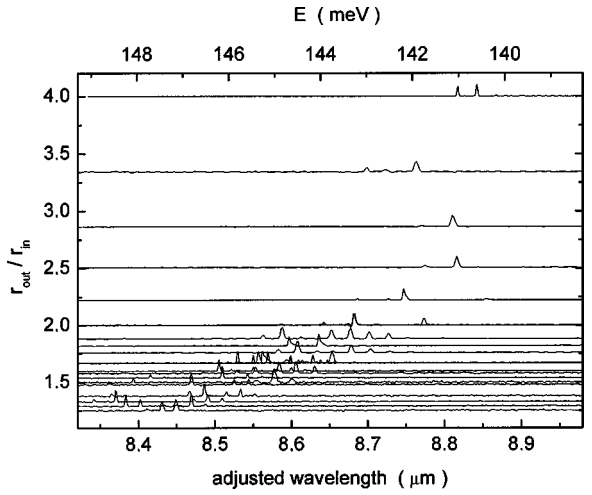

FIG. 2. Spectra of rings with outer radii of 100, 150, and 200 μm and various inner radii. The spectra were normalized and shifted along the y axis such that the background signal of each spectrum indicates the ratio of its radii. The adjustment of the spectra in the x direction is explained in the text.

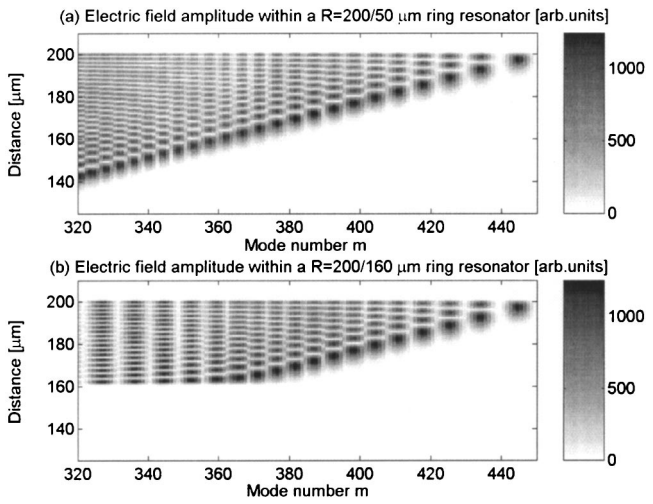

FIG. 3. A FDTD simulation of the electric field amplitude vs distance from the resonator center and mode number. Results are presented for 50 μm (a) and 160 μm (b) inner ring radius. The outer radius was fixed at 200 μm for both simulations. The simulations were performed within a small amplitude approximation. To simulate a narrow gain-loss spectrum, a central frequency of 35 THz and a dephasing time of 1 ps were used.

the threshold in ring cavities is presumably caused by small irregularities in the cavities. Fabry-Pérot cavities with cleaved facets possess more regular mirrors. The spectra discussed in the following were taken at 78 K. Most ring lasers showed lasing up to at least 270 K; selected devices lased at room temperature. The spectra in Fig. 2 were taken at a bias of approximately twice the threshold current. Each spectrum shows several modes. The mode spacing is clearly not regular, which would be expected for ideal rings.

A striking feature of the spectra is their blueshift with increasing inner radius. Figure 2 shows spectra for three different outer and various inner radii. Since the emission wavelength also shifts with outer radius (not shown), the emission wavelengths of the rings with outer radii of 150 and 200 μm were manually blueshifted by a constant of 0.14 and 0.27 μm, respectively. The constants were obtained from spectra of devices with a ratio $r_{\mathrm{out}}/r_{\mathrm{in}}=1.67$, because this is the only ratio where spectra from devices with all three outer radii were measured. The spectra were further shifted along the y axis so that the background signal indicates the ratio $r_{\mathrm{out}}/r_{\mathrm{in}}$. The observed blueshift is not correlated to the threshold or to the position on the wafer. While we observed different optical modes if the system was thermally cycled and also if the signal was detected with the ring rotated, the envelope of the individual modes did not change. Interestingly, the spectra do not blueshift for small inner radii. The spectra start to shift for a ratio of the radii $r_{\mathrm{in}}/r_{\mathrm{out}}\approx 0.43$. Apparently, the mode distribution does not extend to the inner rim for sufficiently small inner radii. Within a simple ray model, it follows from trigonometry that modes propagating by total internal reflection never penetrate a circle of radius $r_{\mathrm{out}}\sin\chi$ (named the ''caustic''). χ is the angle of total internal reflection of the material, $\chi=\sin^{-1}(1/n_{\mathrm{eff}})$. Normal incidence corresponds to 0°. An estimate of $n_{\mathrm{eff}}=3.17$ from a distributed feedback laser processed from a similar material as our ring lasers yields $\chi=18.4°$. From these considerations, the modes are not cut off below a ratio of $r_{\mathrm{in}}/r_{\mathrm{out}}=0.32$, which is not too far from the experimental value. Thus, it appears that the blueshift is caused by the interaction of the lasing modes with the inner rim of the ring.

We now turn to the simulations. We have applied the body of revolution finite-difference time-domain (BOR FDTD) method[16] coupled with the finite-difference algorithm for two level atoms similar to the one suggested in Ref. 17 to obtain a distribution of the electromagnetic field in ring-shaped QCL resonators. Within the BOR FDTD algorithm, fields are expanded in a Fourier series of sines and cosines:

$$\vec{E}=\sum_{m=0}^{\infty}(\vec{e}_u\cos m\phi+\vec{e}_v\sin m\phi),$$

$$\vec{H}=\sum_{m=0}^{\infty}(\vec{h}_u\cos m\phi+\vec{h}_v\sin m\phi),$$

where the mode number m is the number of wavelengths per circumference. The solution is obtained for each mode separately.

For each number m an initial wave with an amplitude of one arbitrary unit was ''injected'' into the entire area of the waveguide. Then the FDTD algorithm was executed to obtain a steady electromagnetic field energy distribution. Afterward, all field components were normalized by dividing them by the value of the amplitude at the maximum point. These values served as new initial values for the second FDTD simulation. The FDTD algorithm was then executed again to obtain the amplitude distributions presented in Fig. 3. Clear intensity maxima are obtained when the frequencies of the resonant modes of the ring match the gain maximum, which is specified in the FDTD at 8.86 μm. As expected, first order radial modes with high amplitudes appear for mode numbers above 440. Interestingly, the amplitudes of

higher order modes are comparable to the amplitudes of first order modes. This may be compared to measurements of the lasing intensity distribution in a pendant drop.[18] It was found that the modes take up the entire annulus between the caustic and the outer rim. In particular, we find that intensity distributions of modes with mode numbers lower than 380 are strongly affected by the presence of the inner border [Fig. 3(b)].

The appearance of higher order modes is unexpected because first order modes are expected to have the lowest losses. Experimental evidence for these modes, commonly known as whispering gallery modes, has been extracted from the mode spacing in circular cavities.[5–8,19–21] Our experiments and simulations suggest that in addition to first order modes, higher order modes extend toward the center of the ring. This result can be understood if we take into account the high gain of mid-IR QCLs and the low loss at the outer rim of the rings. (For example, Hagness *et al.*[1] found *Q'*s of several thousands for their circular semiconductor microcavities.) For sufficiently high gain, the electromagnetic field amplitude is nearly unaffected by variations of the loss at the outer boundary. In fact, irregularities in the gain distribution due to the fabrication process can have a greater influence on the appearance of higher order modes than losses at the rim. As a result, many modes are expected within the rings.

The transition between disk and ring resonators has also been treated with finite-difference time-domain microcavity simulations by Hagness *et al.*[1] It was found that, as the inner radius of the ring is increased, each set of resonances (i.e., a mode with the same number of nodes) shifts toward smaller wavelengths. Moon *et al.*[22] investigated a blueshift of whispering gallery modes that was caused by a decrease of their cavity *Q* when the refractive index was decreased thermally. Corbett *et al.*[6] found that the lasing wavelength of InGaAs quantum well microring lasers decreases as the ring size decreases. Here, the wavelength shift is explained by higher carrier densities required to match the higher curvature losses and the reduced gain length. This implies that the emission wavelength depends on the bias. We have confirmed on our samples that the wavelength shift with bias is only minimal.

To summarize, we have studied the spectra of mesoscopic ring lasers processed from a quantum cascade material. This work investigates the influence of the inner rim on the spectral behavior of ring lasers. From the observed blueshift of the spectra for inner radii beyond approximately 43% of the outer radius, we conclude that in this range the optical modes interact with the inner rim. In agreement with the experiments, simulations show that the electric field for higher order modes, which are affected by the presence of the inner ring border, is comparable to the electric field of the first order mode.

We would like to thank J. Darmo and C. Pflügl for helpful discussions and P. Schwaha for performing some of the measurements. This work was supported by the European Community–IST project SUPERSMILE, by the Austrian Microelectronics Society, and by the Austrian FWF.

[1] S. C. Hagness, D. Rafizadeh, S. T. Ho, and A. Taflove, J. Lightwave Technol. **15**, 2154 (1997).
[2] B. E. Little, S. T. Chu, W. Pan, and Y. Kokubun, IEEE Photonics Technol. Lett. **12**, 323 (2000).
[3] D. K. Armani, T. J. Kippenberg, S. M. Spillane, and K. J. Vahala, Nature (London) **421**, 925 (2003).
[4] H. J. Moon, Y. T. Chough, and K. An, Phys. Rev. Lett. **85**, 3161 (2000).
[5] Y. Kawabe, C. Spiegelberg, A. Schülzgen, M. F. Nabor, B. Kippelen, E. A. Mash, P. M. Allemand, M. Kuwata-Gonokami, K. Takeda, and N. Peyghambarian, Appl. Phys. Lett. **72**, 141 (1998).
[6] B. Corbett, IEEE Photonics Technol. Lett. **10**, 3 (1998).
[7] K. C. Zeng, L. Dai, J. Y. Lin, and H. X. Jiang, Appl. Phys. Lett. **75**, 2563 (1999).
[8] B. Corbett, P. Lambkin, G. H. Wu, J. Houlihan, and G. Huyet, Appl. Phys. Lett. **81**, 808 (2002).
[9] J. Faist, C. Gmachl, M. Striccoli, C. Sirtori, F. Capasso, D. L. Sivco, and A. Y. Cho, Appl. Phys. Lett. **69**, 2456 (1996).
[10] C. Gmachl, F. Capasso, E. E. Narimanov, J. U. Noeckel, A. D. Stone, J. Faist, D. L. Sivco, and A. Y. Cho, Science **280**, 1556 (1998).
[11] S. Gianordoli, L. Hvozdara, G. Strasser, W. Schrenk, K. Unterrainer, and E. Gornik, Appl. Phys. Lett. **75**, 1045 (1999).
[12] S. Anders, W. Schrenk, E. Gornik, and G. Strasser, Appl. Phys. Lett. **80**, 4094 (2002).
[13] A. Mekis, J. U. Nöckel, G. Chen, A. D. Stone, and R. K. Chang, Phys. Rev. Lett. **75**, 2682 (1995).
[14] S. Gianordoli, L. Hvozdara, G. Strasser, W. Schrenk, J. Faist, and E. Gornik, IEEE J. Quantum Electron. **36**, 458 (2000).
[15] W. Schrenk, E. Gornik, H. Page, C. Sirtori, V. Ortiz, and G. Strasser, Physica E (Amsterdam) **13**, 840 (2002).
[16] A. Taflove, *Computational Electrodynamics: The Finite-Difference Time-Domain Method* (Artech House, Norwood, Massachusetts, 1995).
[17] R. W. Ziolkowski, J. M. Arnold, and D. M. Gogny, Phys. Rev. A **52**, 3082 (1995).
[18] X. Y. Pu, C. W. Chan, and W. K. Lee, Opt. Lett. **25**, 1514 (2000).
[19] A. F. J. Levi, R. E. Slusher, S. L. McCall, S. J. Pearton, and W. S. Hobson, Appl. Phys. Lett. **62**, 2021 (1993).
[20] M. J. Ries, E. I. Chen, N. Holonyak, Jr., G. M. Iovino, and A. D. Minervini, Appl. Phys. Lett. **68**, 1540 (1996).
[21] R. A. Mair, K. C. Zeng, J. Y. Lin, H. X. Jiang, B. Zhang, L. Dai, A. Botchkarev, W. Kim, H. Morkoc, and M. A. Khan, Appl. Phys. Lett. **72**, 1530 (1998).
[22] H. J. Moon, Y. T. Chough, J. B. Kim, K. An, J. Yi, and J. Lee, Appl. Phys. Lett. **76**, 3679 (2000).